

## Article

# Numerical modeling of ink widening and coating gap in roll-to-roll slot-die coating of solid oxide fuel cell electrolytic layer

Seongyong Kim<sup>a</sup>, Jongsu Lee<sup>b</sup>, Minho Jo<sup>a</sup>, Changwoo Lee<sup>c,\*</sup>

<sup>a</sup>Department of Mechanical Design and Production Engineering, Konkuk University, 120, Neungdong-ro, Gwangjin-gu, Seoul, 05029, South Korea; arsen6788@gmail.com

<sup>b</sup>Department of Printed Electronics Engineering, Sunchon National University, 255, Jungang-ro, Suncheon, Jeollanam-do, 540-950, South Korea; ljs8755@gmail.com

<sup>c</sup>Department of Mechanical Engineering, Konkuk University, 120, Neungdong-ro, Gwangjin-gu, Seoul, 05029, South Korea; rnjstk1234@gmail.com

\*Corresponding Author E-mail: leewoo1220@konkuk.ac.kr

**Abstract:** Slot-die coatings are advantageous when used for coating large-area flexible devices; in particular, the coating width can be controlled, and simultaneous multi-layer coatings can be processed. Till date, the effects of ink widening and coating gap on the coating thickness have only been considered in a few studies. To this end, we developed two mathematical models to accurately estimate the coating width and thickness considering these two effects. We used root mean square deviation (RMSD) to experimentally verify the developed method. The coating width was seen to increase and the coating thickness was seen to decrease when the coating gap was increased. Experimental results showed that the estimation performances of the coating width and thickness models were as high as 98.46 % and 95.8 %, respectively. We believe that the developed models can be useful for determining the coating conditions according to the ink properties to coat a functional layer with user-defined widths and thicknesses in both lab- and industrial-scale roll-to-roll slot-die coating processes.

**Keywords:** flexible functional device; thin film coating; slot-die; surface tension; coating gap

## 1. Introduction

The roll-to-roll manufacturing process (R2R process) has become a subject of interest owing to its low cost and mass production capability [1]. With this process, large-area functional layers can be fabricated on a flexible polymer substrate using various printing or coating techniques such as blade coating, spray coating, and slot-die coating [2–4]. In particular, slot-die coating has the advantages of controlling the coating width by changing the design of a shim plate assembled in the slot-die chamber and simultaneously processing multi-layer coatings. These can contribute to a decrease in the production costs of flexible electronic devices. Thus, slot-die coating is a good candidate to coat large-area flexible devices on polymer substrates [5], and numerous research groups have studied the fabrication of such devices namely photovoltaic and fuel cells [10–11].

Recently, an electrolytic layer, which is a separator in a solid oxide fuel cell (SOFC), was fabricated using the R2R slot-die coating process. Many studies have analyzed ink behavior in the slot-die coating process and reported the fabrication of single and multi-functional layers using a slot-die coater. In particular, Ruschak et al. [6] established the desired ranges for coating parameters, such as the coating speed, surface tension on ink, and the pressure applied to the inlet and outlet of the coating bead, to obtain a high-quality slot-die coating. Lee et al. [7] analyzed the effects of the geometry of a slot-die coater and coating gap on the coating thickness. Ning et al. [8] studied the change in the coating quality according to the concentration of polymer particles in a coated solution. They determined that the maximum coating speed is dependent on the polymer concentration. Cavalho et al. [4] studied the correlations among the coating gap, Reynolds number, and capillary

number, which are determined by the ink properties such as the density, surface tension, and viscosity of the solution. Yang et al. [9] found a thicker coated layer when the density and viscosity of the coated solution are high. Lee et al. [13] proposed a method to prevent cracks during the brittle electrolytic layer coating using the R2R process. Park et al. [14] developed a technique to alleviate a pinned edge in the coated layer in the R2R slot-die coating process. Kim et al. [15] analyzed the ink velocity profile at the tip of a slot-die coater using finite element analysis and suggested a desired geometry of the same for improving the uniformity of the coating layer. From previous studies, one can see that the behavior of the slot-die coater has been studied using volumetric [16] and visco-capillary models [17]. The volumetric model is based on the continuity equation between the tip of the slot-die coater and the surface of the substrate, which estimates the thickness of the coated layer according to the layer geometry and flow rate of an ink supplier, such as the mono- and syringe pump. The effects of the ink widening determined by its surface tension, surface energy of the substrate, and coating gap are, however, not considered. On the contrary, in the viscocapillary model, the minimum permissible coating thickness that can form a stable coating bead can be estimated by considering the ink properties and coating gap. This model can be used in low-viscosity solution coatings; however, an actual wet coating thickness cannot be estimated. To accurately estimate the thickness of a coated layer, the effects of ink widening and the coating gap on the coating thickness should be considered. However, only a few studies have considered these two effects to estimate the coating thickness in the slot-die coating process. In this paper, we proposed an advanced model based on the volumetric model that can estimate the width and thickness of the coated layer considering the aforementioned effects. The developed method was experimentally verified using root mean square deviation (RMSD), which is generally used to numerically evaluate the estimation performance of theoretical and experimental models.

## 2. Mathematical modeling

Figure 1 presents the flow chart for estimating the coated width and thickness using the coating gap and ink properties such as density, viscosity, and surface tension. The entire process was carried out in five steps.

**Step 1.** Measure the ink properties: viscosity, density, and surface tension of ink.

**Step 2.** Measure the contact angle in the absence of injection height.

**Step 3.** Calculate the volume of injected ink and shape factor to determine the widened length of the droplet of ink [19].

**Step 4.** Calculate the widened length and the ratio of the change of the droplet radius of ink deposited on a substrate ( $r(t) - r_e$ ) to the ink droplet radius at 0 mm of injection height ( $r_e$ ) (named widening ratio,  $wr$ ) using Eq. (1) and Eq. (2), respectively.

**Step 5.** Calculate the coated layer width and thickness (named coating width and coating thickness, respectively) using Eq. (3) and Eq. (5), respectively.

Figures 2 and 3 show schematics of the change in the contact angle and coating width by varying the injection height and the coating gap, respectively. Generally, the ink widening in a tensioned web varies according to the injected volume of ink, injection height, and surface tension [18]. The droplet radius of the ink according to the injection height can be obtained using Harth's model [19] as shown in Eq. (1),

$$r(t) = r_e \left[ 1 - \exp \left( \frac{2\gamma_L}{r_e^{12}} + \frac{\rho g}{9r_e^{10}} \right) \frac{24\lambda v^4(t+t_0)}{\pi^2 \eta} \right]^{\frac{1}{6}} \quad (1)$$

where  $\eta$  is the ink viscosity,  $\lambda$  is the shape factor,  $\gamma$  is the surface tension of ink,  $v$  is the volume of

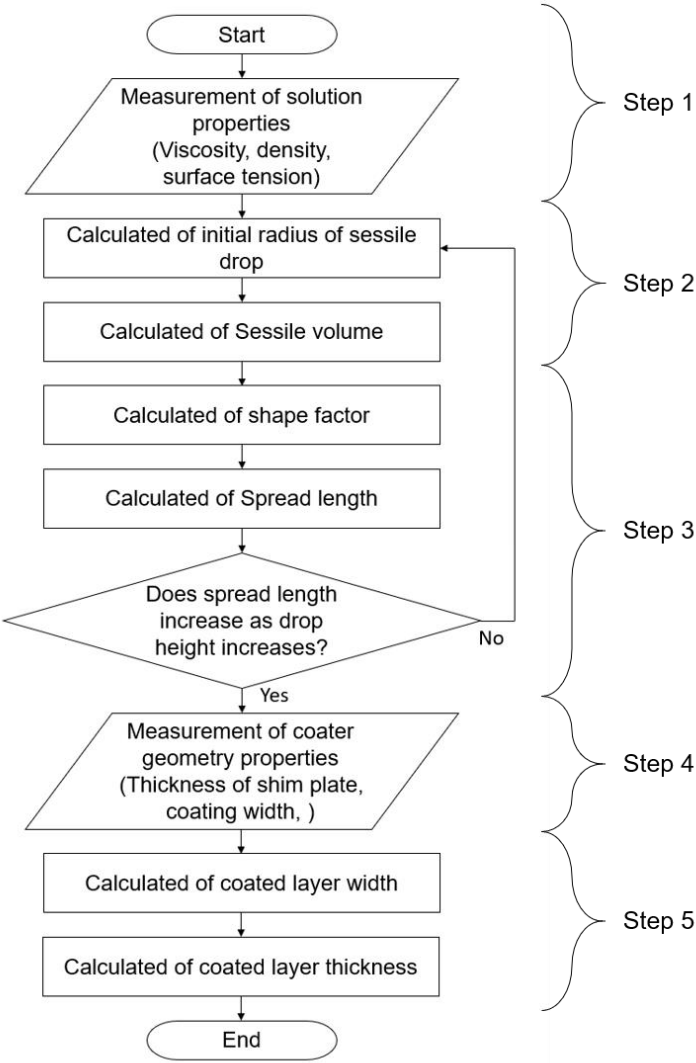


**Figure 1.** Flow chart for estimating the coated width and thickness using the coating gap and ink properties

injected ink,  $r_e$  is the effective radius of the droplet,  $t$  is the time interval between the ink injection and ink deposition on the substrate, and  $g$  and  $\rho$  are the gravitational acceleration and ink density, respectively.

It can be seen that the widened length of the ink, that is, the increase in the radius of the ink, increases with the increasing ink density and injection height, which suggests that the coating width changes according to the coating gap, as shown in Figure 3.

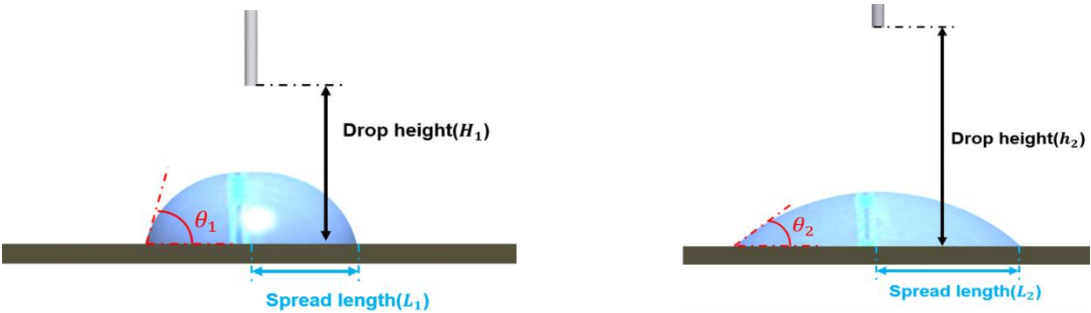


**Figure 2.** Schematics of the change in the contact angle and coating width by varying the injection height

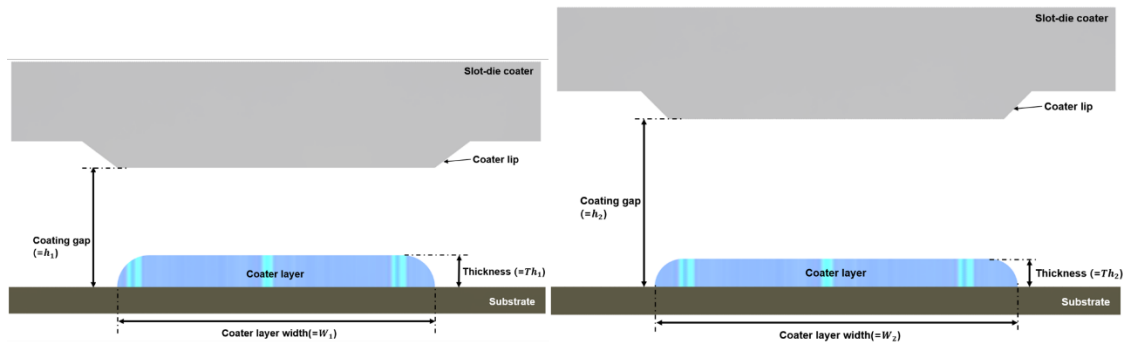


Figure 3. Schematics of the change in the contact angle and coating width by varying the coating gap

Based on Harth's model, we developed a mathematical model to estimate the coating width. The widening ratio ( $wr$ ) can be expressed as Eq. (2)

$$wr = \frac{r(t) - r_e}{r_e} wr = \frac{r(t) - r_e}{r_e} \quad (2)$$

The coating width can be obtained using Eq. (3) considering the width of the slot-die coater, which is the same as the coating width in the absence of the widening effect, and the widening ratio obtained by substituting Eq. (1) in Eq. (2).

$$w(h) = w_0 + (w_0 * wr(h)) \quad (3)$$

where  $w_0$  is the width of the slot-die coater, and  $h$  is the coating gap.

The coating width considering the widening effect can be estimated using Eq. (3). Eq. (4) represents the coating thickness model developed in our previous studies for estimating the coating thickness considering the widening effect [20].

$$th_{e,d} = s(th_{e,w}) = \frac{sKf_r}{nwV} \quad (4)$$

where  $d$  is the thickness of the dried coated layer,  $s$  is the density of the solute of the ink,  $w$  is the thickness of the wet coated layer,  $f_r$  is the flow rate,  $n$ ,  $w$ , and  $V$  are the number of strips of the coated layer, width of the unit strip, and web speed, respectively;  $K$  is a dimensionless number expressing the severity of the widening effect [18, 19]. This model is based on the mass conservation law derived between the tip of the slot-die coater and the surface of the substrate. However, we did not consider the effect of the coating gap in our model.

The coating thickness model considering the widening effect and the change in width according to the coating gap can be obtained using Eq. (5), which is derived by substituting Eq. (3) in Eq. (4).

$$th_{e,d} = \frac{sKf_r}{nw(h)V} = \frac{sKf_r}{n(w_0 + (w_0 * wr(h)))V} \quad (5)$$

### 3. Experimental verification

#### 3.1. Experimental conditions

Yttria-stabilized zirconia (YSZ, Sigma Aldrich, USA), an electrolytic layer of a SOFC, and a dielectric layer (BaTiO<sub>3</sub>, Paru Co. Ltd., South Korea) were coated using a slot-die coater to experimentally verify the developed coating width and thickness models shown in Eqs. (3) and (5), respectively. Table 1 shows the properties of YSZ and of the dielectric solution, while Table 2 lists the coating conditions. A mixture of ethanol and toluene (3:7) and acetone were used as the solvents of YSZ and the dielectric solution, respectively. An industrial-scale R2R slot-die coating machine (Toba Co. Ltd., South Korea), which is shown in Figure 4(a), was used to coat the two materials. The tension and web speed were set to 2.7 kgf and 1 m/min, respectively.

Table 1. Properties of YSZ and of the dielectric solution

Properties	Value	
Solution	Dielectric solution	YSZ solution
Radius of sessile( $r_e$ )	0.167 mm	0.187 mm
Surface tension of solution	26.68 N/mm	28.52 N/mm
Viscosity	0.08 Pa*s	0.03 Pa*s

Table 2. Coating conditions

Process condition	Value
Tension	2.7 kgf
Web speed	1 m/min
Width of Coater	120 mm
Coating gap	100 ~ 500 $\mu$ m

3.2. Experimental results

Figures 4(b) and (c) show the coated layer of YSZ and the dielectric layer, respectively. Each layer was coated 3 times using 9 different values of coating gaps (100–500  $\mu$ m with a 50  $\mu$ m coating gap interval). Figures 5(a) and (b) show the results of measuring the YSZ and dielectric layers using an interferometer (NS-E1000, Nanosystem Co. Ltd., South Korea), respectively.

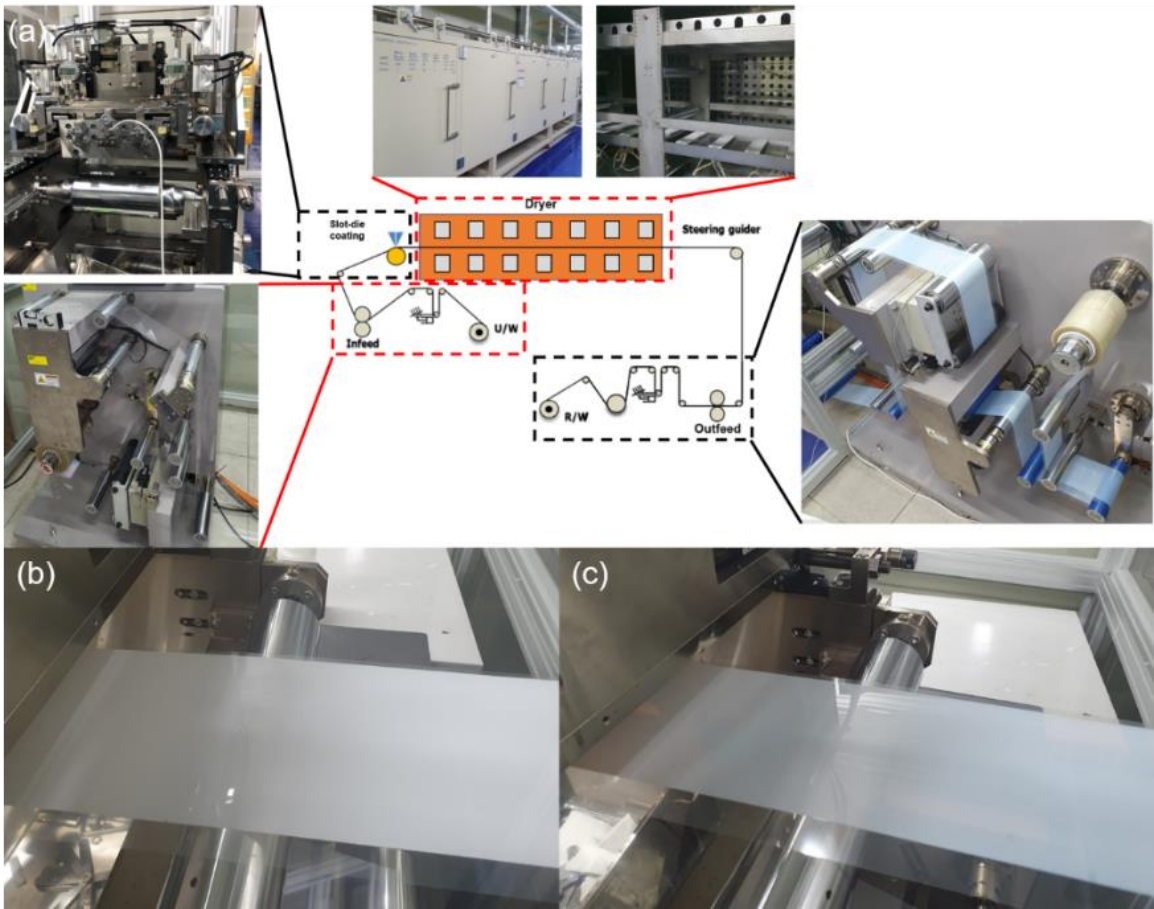
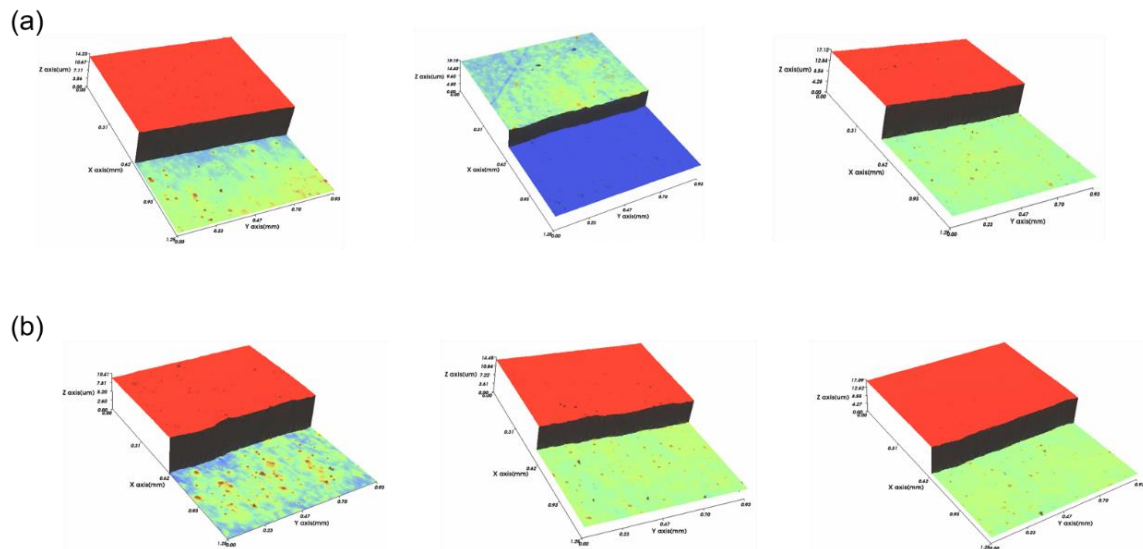


Figure 4. (a) Industrial-scale R2R slot-die coating machine in this study (Toba Co. Ltd., South Korea), (b) the coated layer of YSZ and (c) the dielectric layer





**Figure 5. (a) YSZ and (b) dielectric layers measured using an interferometer (NS-E1000, Nanosystem Co. Ltd., South Korea)**

We compared the measured and estimated thicknesses using the developed models to clearly verify their performance. Tables 3 and 4 show the measured and estimated coating width and thickness of the dielectric and YSZ layers, respectively. Figure 6(a) and (b) presents the measured and estimated width and thickness of the dielectric layer, respectively, while Figure 6(c) and (d) presents the corresponding values of the YSZ layer. It can be seen that the coating width increases and the coating thickness decreases when the coating gap is increased. These results suggest that the widening effect increases with the coating gap. Since the widening effect also increases by increasing the time interval (t) between the ink injection and its deposition, it can also increase the width, thereby increasing the coating gap [17]. The inertia of the ink affects the ink widening more dominantly at higher injection heights.

**Table 3. Measured and estimated coating width and thickness of the dielectric**

Coating gap [ $\mu\text{m}$ ]	Width of coated layer[mm]		Thickness of coated layer[ $\mu\text{m}$ ]	
	Estimated	Measured	Estimated	Measured
100	121.97	122.26	13.66	13.42
150	122.15	122.36	13.64	13.31
200	122.36	122.86	13.62	13.21
250	122.42	123.15	13.61	13.18
300	122.66	123.51	13.58	13.17
350	123.13	123.73	13.54	13.16
400	123.40	124.09	13.50	13.09
450	123.61	124.30	13.48	13.11
500	123.88	124.90	13.54	13.22

Moreover, it is seen that the trends of the estimated width and thickness are similar to the measured ones. The estimation performances of the developed models were evaluated using root mean square deviation (RMSD), which is generally used to numerically evaluate the similarity of approximation values with actual values in the time domain, as shown in Eq. (6).

$$MA(\%) = \sqrt{\frac{\sum_{i=1}^n (x_{measured,i} - x_{estimated,i})^2}{n}} \quad (6)$$

Table 4. Measured and estimated coating width and thickness of the YSZ layer

Coating gap [ $\mu\text{m}$ ]	Width of coated layer[mm]		Thickness of coated layer[ $\mu\text{m}$ ]	
	Estimated	Measured	Estimated	Measured
100	126.48	124.25	15.45	16.54
150	128.04	124.9	15.26	16.36
200	129.24	125.36	15.12	16.19
250	130.32	126.17	14.99	15.83
300	131.4	127.4	14.87	15.74
350	132.24	128.48	14.78	15.68
400	133.08	129	14.69	15.57
450	133.92	130.25	14.59	15.43
500	134.76	131.55	14.50	14.94

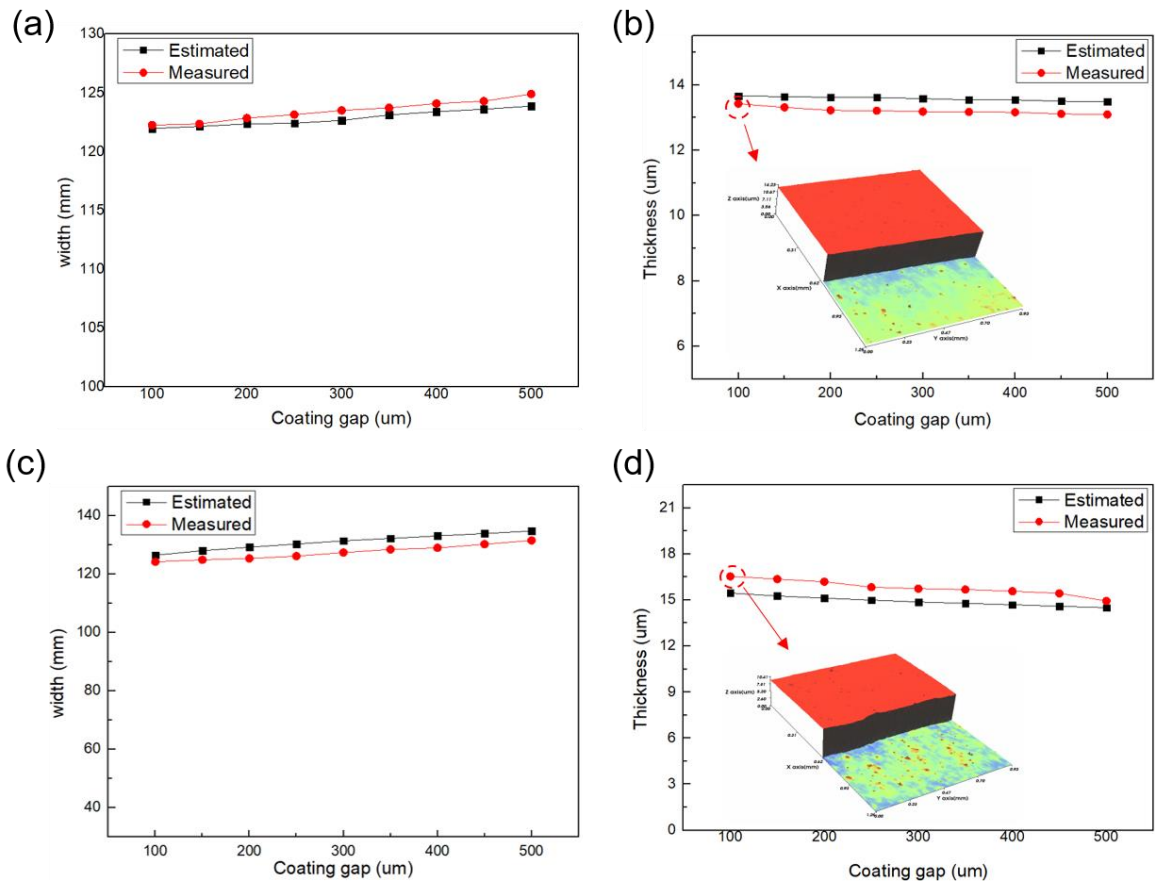


Figure 6. (a) Measured and estimated width and (b) thickness of the dielectric layer, and (c) measured and estimated width and (d) thickness of the of the YSZ layer.

where MA represents the model accuracy, n is the number of the measurements, and  $x_{\text{measured},i}$  and  $x_{\text{estimated},i}$  are the  $i^{\text{th}}$  measured and estimated data, respectively.

**Table 5. Estimation accuracy of the developed coating width and thickness models for the dielectric and YSZ layer coating.**

Coating gap [ $\mu\text{m}$ ]	Accuracy of dielectric solution [%]		Accuracy of YSZ solution [%]	
	Width	Thickness	Width	Thickness
100	99.76	98.21	98.21	92.95
150	99.83	97.52	97.49	92.79
200	99.88	96.97	96.91	92.93
250	99.64	96.97	96.71	94.4
300	99.61	96.97	96.86	94.15
350	99.71	97.04	97.07	93.91
400	99.6	97.11	96.84	94.01
450	99.44	97.03	97.19	98.98
500	99.98	97.02	97.56	96.97

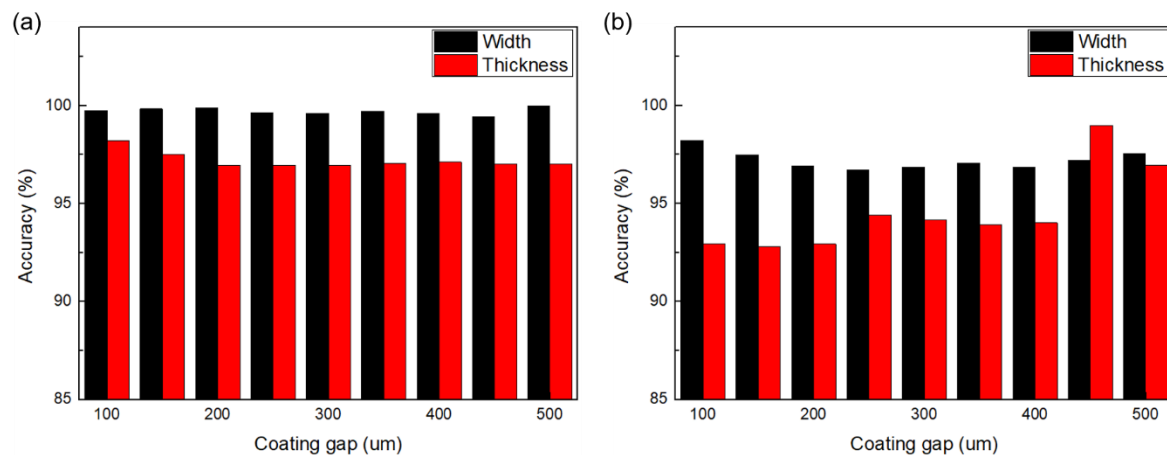
**Figure 7. Estimation accuracy of the developed coating width and thickness models for (a) the dielectric and (b) YSZ layer coating.**

Table 5 and Figure 7 present the estimation accuracy of the developed coating width and thickness models for the dielectric and YSZ layer coating. One can see that the average estimation accuracies of the coating width and thickness models are 98.46 % and 95.8 %, respectively, which demonstrates the superiority of these models.

#### 4. Conclusion

We developed two mathematical models to estimate the coating width and thickness considering the coating gap and widening effect of ink in R2R slot-die coatings. We considered the effect of ink properties and its inertia on the coating width and thickness according to the coating gap in our models. We coated the YSZ and dielectric layers using an industrial-scale R2R slot-die coater to experimentally verify the superiority of the developed models, whose estimation performances were then verified using the RMSD method. Experimental results show estimation performances of the coating width and thickness models to be 98.46 % and 95.8 %, respectively. We believe the developed model can be useful for determining the coating conditions according to the ink properties to coat a functional layer with user-defined widths and thicknesses in both lab- and industrial-scale R2R slot-die coating processes.



**Author Contributions:** Conceptualization, S.K and C.L.; data curation, M.J.; Formal Analysis, S.K. and M.J.; writing—original draft preparation, S.K. and C.L.; supervision, J.L. and C.L.; project administration, C.L.; Writing-Review & Editing J.L. and C.L.; Funding Acquisition, C.L. All authors have read and agreed to the published version of the manuscript.

**Acknowledgments:** This work was supported by a National Research Foundation of Korea grant funded by the Korean government (MSIT) (No. 2020R1A2C1012428).

**Conflicts of Interest:** Declare conflicts of interest or state “The authors declare no conflict of interest.” Authors must identify and declare any personal circumstances or interest that may be perceived as inappropriately influencing the representation or interpretation of reported research results. Any role of the funders in the design of the study; in the collection, analyses or interpretation of data; in the writing of the manuscript, or in the decision to publish the results must be declared in this section. If there is no role, please state “The funders had no role in the design of the study; in the collection, analyses, or interpretation of data; in the writing of the manuscript, or in the decision to publish the results”.

## References

1. Lee, J.; Byeon, J.; Lee, C. Theories and control technologies for web handling in the roll-to-roll manufacturing process. *Int. J. Precision Engg. & Manuf-Green Techno.* **2020**, *7*, 525–544.
2. Kapur, N. A parametric study of direct gravure coating. *Chemical Engg. Sci.* **2003**, *58*, 2875–2882.
3. Tseng, S-R et al. Multilayer polymer light-emitting diodes by blade coating method. *Appl. Phys. Lett.* **2008**, *93*, 382.
4. Carvalho, M.S.; Haroon S.K. Low-flow limit in slot coating: Theory and experiments." *AIChE J.* **2004**, *46*, 1907–1917.
5. Lin, C-F.; Wong, D.S.H.; Liu, T-J.; Wu, P-Y. Operating windows of slot die coating: Comparison of theoretical predictions with experimental observations. *Advances in Polymer Technol.: J. Polymer Processing Institute* **2010**, *29*, 31–44.
6. Ruschak, K.J. Limiting flow in a pre-metered coating device. *Chemical Engg. Sci.* **1976**, *31*, 1057–1060.
7. Lee, K-Y.; Liu, L-D.; Liu, T-J. Minimum wet thickness in extrusion slot coating. *Chemical Engg. Sci.* **1992**, *47*, 1703–1713.
8. Ning, C-Y.; Tsai, C-C.; Liu, T-J. The effect of polymer additives on extrusion slot coating. *Chemical Engg. Sci.* **1996**, *51*, 3289–3297.
9. Yang, C.K.; Wong, D.S.H., Liu, T. J. The effects of polymer additives on the operating windows of slot coating. *Polymer Engg. & Sci.* **2004**, *44*, 1970–1976.
10. Lee, K; JS Spendelow; Choe Y; C Fujimoto; Kim Y. An operationally flexible fuel cell based on quaternary ammonium-biphosphate ion pairs. *Nat Energy.* **2016**, *1*, 9, 16120
11. K Tran; TQ Nguyen; AM Bartrom; A Sadiki; JL Haan. A fuel-flexible alkaline direct liquid fuel cell. *Fuel Cells.* **2014**, *14*, 6, 834–841
12. Krebs, F.C.; Jan, F.; Jørgensen, M. Product integration of compact roll-to-roll processed polymer solar cell modules: methods and manufacture using flexographic printing, slot-die coating and rotary screen printing. *J. Materials Chem.* **2010**, *20*, 8994–9001.
13. Lee, J.; Kim, S.; Lee, C.; Surface drying for brittle material coating without crack defects in large-area roll-to-roll coating system. *Int. J. Precision Engg. & Manuf-Green Techno* **2019**, *6*, 723–730.
14. Park, J.; Kim, S.; Lee, C.; An analysis of pinned edge layer of slot-die coated film in roll-to-roll green manufacturing system. *Int. J. Precision Engg. & Manuf-Green Techno* **2018**, *5*, 2, 247–254.
15. Kim, S.; Lee, J.; Lee, C. Computational fluid dynamics model for thickness and uniformity prediction of coating layer in slot-die process. *The Int. J. of Advanced Manuf. Technol.* **2019**, *104*, 2991–2997.
16. Kang, H.; Park, J.; Shin, K. Statistical analysis for the manufacturing of multi-strip patterns by roll-to-roll single slot-die systems. *Robotics & Computer-Integrated Manuf.* **2014**, *30*, 363–368.
17. Higgins, B.G.; Lawrence, E.S. Capillary pressure and viscous pressure drop set bounds on coating bead operability. *Chemical Engg. Sci.* **1980**, *35*, 673–682.
18. Park, J.; Kim, D.; Lee, C. Contact angle control of sessile drops on a tensioned web. *Appl. Surface Sci.* **2018**, *437*, 329–335.
19. Harth, M.; Schuber, D.W. Simple approach for spreading dynamics of polymeric fluids. *Macromolecular Chem. & Phys.* **2012**, *213*, 654–665.

20. Lee, J.; Kim, S.; Lee, C. Large area electrolyte coating through surface and interface engineering in roll-to-roll slot-die coating process. *J. Industrial & Engg. Chem.* **2019**, *76*, 443–449.
21. Lee, J.; Byeon, J.; Lee, C.; Fabrication of thickness-controllable double layer electrolyte using roll-to-roll additive manufacturing system. *Int. J. Precision Engg. & Manuf-Green Techno* **2020**, *7*, 635–642.